Steady longitudinal motion of a cylinder in a conducting fluid

By HIDENORI HASIMOTO
Department of Aeronautics, The Johns Hopkins University*

(Received 4 September 1959)

The steady motion of an infinitely long solid cylinder parallel to its length in a conducting fluid in the presence of a uniform magnetic field is discussed. Due to Alfvén waves originating at the cylinder we find two opposite 'wakes' parallel to the applied magnetic field.

A formula which relates the total drag on the cylinder to the electric potential difference $\delta\Phi$ between the two undisturbed regions outside these two wakes is derived

$$D/|\delta\Phi| = 2\sqrt{\rho\nu\sigma},$$

where $\rho\nu$ is the viscosity and σ is the conductivity of the fluid.

The reduction to a classical boundary-value problem is made for the case of an insulating cylinder.

Exact solutions are obtained for the case of a perfectly conducting or an insulating flat strip of semi-infinite width. These give a clear picture of the fields, especially in the transition region near the edge of the strip.

The case of a strip of finite width is also discussed with special reference to the viscous and the magnetic drags, D_f and D_m. We find that $D_f + \frac{1}{2}D_m$, on a perfectly conducting strip, is equal to the viscous drag on an insulating strip for which D_m is zero. Precise values of these drags are given.

1. Introduction

There are only a few cases in magneto-hydrodynamics for which exact treatments are possible. A typical case is that of the rectilinear fluid flow in pipes under the uniform transverse magnetic field. The studies initiated by Hartmann (1937) for the flow between two walls have been extended by Shercliff (1953, 1956) to the case of the flow in a straight pipe. Resler & Sears (1958) studied the case of a compressible fluid, neglecting viscosity. Also we should mention the work of Bleviss (1958) on the Couette flow between parallel walls.

As far as the author is aware, problems in which there is an unlimited fluid flow outside a rigid cylinder, corresponding to the above cases, have remained untouched, except for the oscillating flow (Kakutani 1958) and Rayleigh's problem (Rossow 1957; Chang & Yen 1959) for an infinite flat plate. In a study of Rayleigh's problem by the present author it was found that an inhomogeneous stationary field remains near the plate after a long period of time. This field has a boundary-layer structure in which the velocity goes from the speed of the plate

* On leave of absence from Kyoto University, Japan.

to a definite fraction of the plate speed sufficiently far away. This represents residual stationary disturbances from the passage of Alfvén waves along the applied magnetic field, and suggests the existence of non-trivial steady solutions for the case of the longitudinal motion of a cylinder of finite cross-section, even though such solutions do not exist for the case of no magnetic field. In the magnetic case, there will also appear interesting transition regions (B) between the regions (C) influenced by Alfvén waves originating at the cylinder and the outer regions (A) which may not be influenced directly by these waves for large Hartmann number M (figure 1). We will also derive the viscous and the magnetic drags on the cylinder. This is motivated by problems of practical interest, relating to the flight of slender bodies in space.*

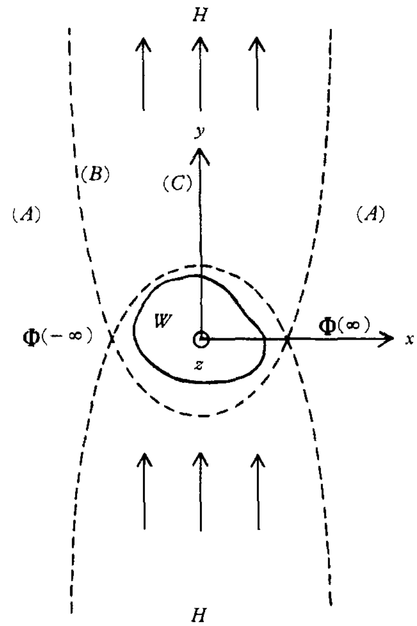

FIGURE 1. Cross-section of cylinder in a transverse magnetic field.

In § 2, we will write down the fundamental equations and the boundary conditions for our problem assuming that the magnetic permeability is the same in the fluid and the cylinder.

In § 3, general characteristics of the problem which allow two 'wakes' (C) in the positive and the negative directions of the applied field will be discussed. We derive a simple formula which relates the drag on the cylinder to the electric potential difference between two undisturbed regions (A) outside these wakes (figure 1). These two quantities are also related to the strength of the wakes at infinity.

We also show that the problem is simplified for the case of an insulating cylinder, since it reduces to a well-known boundary-value problem of mathematical physics.

* Our solutions are also considered to afford limiting fields around a huge annulus rotating slowly about its axis of symmetry, which is parallel to the strong applied magnetic field.

As an example, the problem for a flat strip is considered in §§ 4 and 5. We confine this study to the two cases of (I), insulating, and (II), perfectly conducting plates. In § 4, we reduce our problem to two standard boundary-value problems for the Helmholtz equation, and we give precise numerical values for the viscous and the magnetic drags on the plate.

In § 5, we give the exact solution of our problem for a strip of semi-infinite width. This solution affords a clear picture of the fields, especially in the boundary layer on the insulating plate and in the transition regions between the outer undisturbed region and the inner core region (which has almost the same velocity as the perfectly conducting plate and one-half the velocity of the insulating plate). Also we find the circuit of the induced electric current around this core.

This behaviour is considered to be the limiting behaviour of the field near a cylinder of given finite width, at sufficiently large Hartmann number. Some consideration is given to this configuration including the case of a thin flat plate with finite conductivity. Comparison with the final steady solutions in Rayleigh's problem with magnetic field for an infinite flat plate is made, and there is perfect agreement with a magnetic Prandtl number of 1.

2. Fundamental equations

We shall use m.k.s. units for the electromagnetic quantities and employ conventional notations. Then, the magneto-hydrodynamic equations for a steady incompressible fluid are

$$(\mathbf{V}.\nabla)\,\mathbf{V} = -\frac{1}{\rho}\nabla(p+\tfrac{1}{2}\mu\mathbf{H}^2)+\nu\nabla^2\mathbf{V}+\frac{\mu}{\rho}(\mathbf{H}.\nabla)\,\mathbf{H}, \tag{2.1}$$

$$\nabla.\mathbf{V} = 0, \tag{2.2}$$

$$(\mathbf{V}.\nabla)\,\mathbf{H} = \kappa\nabla^2\mathbf{H}+(\mathbf{H}.\nabla)\,\mathbf{V}, \quad \kappa = 1/(\mu\sigma), \tag{2.3}$$

$$\nabla.\mathbf{H} = 0, \tag{2.4}$$

$$\mathbf{E} = -\mu\mathbf{V}\wedge\mathbf{H}+\mathbf{J}/\sigma, \tag{2.5}$$

$$\mathbf{J} = \nabla\wedge\mathbf{H}, \tag{2.6}$$

in a Cartesian coordinate system (x, y, z), which is at rest with respect to the fluid at infinity.

Let us consider the steady flow due to the uniform longitudinal motion, with velocity W, of an infinitely long cylinder with its generators parallel to the z-axis, in the presence of a uniform magnetic field of strength H parallel to the y-axis. We assume that the magnetic permeability μ of the cylinder is the same as that of the fluid. The suffix i will be used to denote quantities in the cylinder (so that (2.1) and (2.2) should be replaced by $v_{ix} = 0$, $v_{iy} = 0$ and $v_{iz} = W$).

With similar assumptions to those in Shercliff's treatment, we have:

(1) all quantities are independent of z;

(2) the induced velocity and magnetic fields are parallel to the z-axis, i.e. $v_x = v_y = 0$, $H_x = 0$, $H_y = H$, and tend to zero at infinity. Then, (2.1)–(2.4) reduce to two-dimensional equations in the x–y plane

$$p = p_\infty-\tfrac{1}{2}\mu H_z^2, \tag{2.7}$$

$$\nabla^2 w+m(\partial h/\partial y) = 0, \tag{2.8}$$

$$\nabla^2 h+m(\partial w/\partial y) = 0, \tag{2.9}$$

where
$$w = v_z/W, \quad h = mH_z/(\sigma\mu HW), \tag{2.10}$$
$$m = \sqrt{(\mu H^2/\rho)}/\sqrt{\nu\kappa} = \sigma\mu\,|H|/\sqrt{(\rho\nu\sigma)}, \tag{2.11}$$
$$\nabla^2 = \partial^2/\partial x^2 + \partial^2/\partial y^2, \tag{2.12}$$

and p_∞ is the constant fluid pressure at infinity. The electric current density **J** and electric field **E** are also parallel to the (x, y)-plane

$$\mathbf{J} = (\sigma\mu HW/m)\,\mathbf{j} \tag{2.13}$$

and
$$E_x = \mu HW(w + j_x/m), \quad E_y = \mu HW j_y/m, \tag{2.14}$$

where
$$j_x = \partial h/\partial y, \quad j_y = -\partial h/\partial x. \tag{2.15}$$

Equations (2.8) and (2.9) must be solved with the boundary conditions

$$w \to 0, \quad h \to 0 \quad \text{at infinity}, \tag{2.16}$$
$$w = 1 \quad \text{on the surface of the cylinder } S, \tag{2.17}$$
$$h = h_i, \quad \partial h/\partial n = (\sigma/\sigma_i)\,\partial h_i/\partial n \quad \text{on } S, \tag{2.18}$$

where $\partial/\partial n$ is the outward normal derivative on the cylinder, and

$$h_i = mH_{iz}/(\sigma\mu HW) \tag{2.19}$$

is the magnetic field in the cylinder satisfying the induction equation (Maxwell's equation)

$$\nabla^2 h_i = 0, \tag{2.20}$$

derived from (2.9) by putting $w = 1$ and replacing h by h_i.

The condition (2.18) for h needs some elucidation. On the surface of the cylinder, we must satisfy the boundary conditions for the electromagnetic quantities

$$\mathbf{H} = \mathbf{H}_i, \quad \mathbf{E}_s = \mathbf{E}_{is}, \tag{2.21}$$

where the suffix s denotes the tangential component around S, and

$$E_{ix} = \mu HW + (\partial H_{iz}/\partial y)/\sigma_i, \quad E_{iy} = -(\partial H_{iz}/\partial x)/\sigma_i. \tag{2.22}$$

If we take into account (2.10), (2.19), (2.14), (2.17) and (2.22), we find that (2.21) is replaced by (2.18) or

$$\mathbf{J}_n = \mathbf{J}_{in} = \partial \mathbf{H}_z/\partial s, \quad \mathbf{E}'_{is} = \mathbf{J}_s/\sigma = \mathbf{J}_{is}/\sigma_i = (\partial \mathbf{H}_z/\partial n)/\sigma, \tag{2.23}$$

where
$$\mathbf{E}'_i = \mathbf{E}_i - \mu\mathbf{H} \wedge \mathbf{W} = \mathbf{J}_i/\sigma_i \tag{2.24}$$

is the electric field in the co-ordinate system moving with the cylinder. Equation (2.23) yields a kind of refraction relation for the electric current

$$\tan\alpha/\tan\alpha_i = \sigma/\sigma_i, \tag{2.25}$$

where α denotes the angle between the current and the normal to S.

Let us try to eliminate h_i from the problem by replacing (2.18) by a single condition for h. Let P and P_0 be two points on s and $N(P_0; P)$ be the Green function in the Neumann problem for the domain bounded by s. Then

$$h_i(P_0) = \frac{1}{s}\oint_S h_i(P)\,ds + \oint_S N(P_0; P)\frac{\partial h_i(P)}{\partial n}\,ds. \tag{2.26}$$

where s is the total length of S and ds is the line element of S at P. In the second integral of (2.26) we take the principal value. Also

$$\oint_S (\partial h_i(P)/\partial n)\, ds = 0, \tag{2.27}$$

because h_i is a harmonic function.

Introducing (2.18) into (2.26) and (2.27) we obtain

$$h(P_0) = \frac{1}{s}\oint_S h(P)\, ds + \frac{\sigma_i}{\sigma}\oint_S N(P_0; P)\frac{\partial h(P)}{\partial n}\, ds, \tag{2.28}$$

$$\oint_S (\partial h(P)/\partial n)\, ds = \oint_S j_s\, ds = 0. \tag{2.29*}$$

Equation (2.28), in conjunction with (2.29), is the boundary condition to be used instead of (2.18) for general values of σ_i/σ.

Taking into account the boundedness of h and $\partial h/\partial n$ for finite σ, we can reduce the above equations to a more simple form for the following two extreme cases.

(I) Perfectly conducting cylinder: $\sigma_i \to \infty$

$$\partial h/\partial n = 0 \quad (\text{or } j_s = 0) \quad \text{on } S. \tag{2.30}$$

This follows most readily from (2.23) because $\mathbf{E}' = 0$ in the cylinder. In this case the electric current in the fluid at the cylinder is perpendicular to S.

(II) Insulating cylinder: $\sigma_i \to 0$

$$h = h_i = \text{const.} \quad \text{in and on the cylinder} \tag{2.31}$$

with

$$\oint_S (\partial h/\partial n)\, ds = 0. \tag{2.32}$$

If the cylinder is symmetric with respect to some (x, z)-plane h_i is zero (see (3.23)). For the general asymmetric case, or if there is more than one cylinder, (2.32) seems to be necessary to determine h_i uniquely. The result (2·31) is evident when we remember that the electric current must be parallel to the cylinder and that h is the stream function of $\mathbf{j}$.

3. General properties of the fields

Before entering into specific boundary-value problems, we will discuss some properties of the solutions of (2·8) and (2·9), satisfying the conditions at infinity (2.16).

Eliminating w or h we obtain

$$(\nabla^2 - m\partial/\partial y)(\nabla^2 + m\partial/\partial y)(w \text{ or } h) = 0, \tag{3.1}$$

which yields
$$w = \phi_+ + \phi_-, \quad h = -\phi_+ + \phi_-, \tag{3.2}$$

where
$$(\nabla^2 \mp m\partial/\partial y)\,\phi_\pm = 0. \tag{3.3}$$

* (2.29) may be deduced more fundamentally from $\nabla \wedge \mathbf{E} = 0$, i.e. $\oint_S \mathbf{E}_s\, ds = 0$, if we use (2.14) and (2.17).

Introducing
$$\tilde{\phi}_{\pm} = \phi_{\pm} \exp(\mp ky), \tag{3.4}$$
where
$$k = \tfrac{1}{2}m, \tag{3.5}$$
we get
$$(\nabla^2 - k^2)\tilde{\phi}_{\pm} = 0. \tag{3.6}$$

Equation (3.3) is well known as the Oseen equation (Lamb 1932), which suggests the existence of 'wakes' of vague parabolic shape along positive and negative y-axes at a great distance from the obstacle. This is shown by the general solution satisfying (2.16)

$$\phi_{\pm} = e^{\pm ky}\,\mathrm{Re}\sum_{n=0}^{\infty} A_{n\pm} K_n(kr)\, e^{in(\theta \mp \frac{1}{2}\pi)} \tag{3.7}$$

$$= B_{\pm}\sqrt{\frac{\pi}{2kr}}\, e^{-kr(1\mp\sin\theta)} + O((kr)^{-\frac{3}{2}}) \quad \text{for} \quad kr \gg 1, \tag{3.7'}$$

with
$$B_{\pm} = \mathrm{Re}\sum_{n=0}^{\infty} A_{n\pm}, \tag{3.8}$$

where K_n is the modified Bessel function of order n, and (r, θ) are the cylinder co-ordinates
$$x = r\cos\theta, \quad y = r\sin\theta. \tag{3.9}$$

Notice that $r(1 \pm \sin\theta) =$ const. are the parametric equations for a parabola.

These wakes represent residual stationary disturbances from the passage of Alfvén waves along the $\pm y$-axes ($\theta = \pm\frac{1}{2}\pi$) in the presence of the combined action of viscosity and conductivity of the fluid. In these two 'wakes', given by (3.7),
$$\phi_+ \gg \phi_- \quad \text{or} \quad \phi_+ \ll \phi_- \quad \text{according as} \quad ky \to \pm\infty, \tag{3.10}$$
so that
$$\tfrac{1}{2}\mu \mathbf{H}_z^2 = (\nu/\kappa)\,\tfrac{1}{2}\rho \mathbf{V}^2, \tag{3.11}$$

i.e. there is a simple relation between the induced magnetic energy and the kinetic energy of the fluid, and the electric current flows along the lines $w =$ const.

We now show a simple relation between the drag per unit length of the cylinder and the difference $\delta\Phi$ between the electric potential at $x = +\infty$ and $x = -\infty$ (for fixed y). Except for a constant, the electric potential Φ is a single-valued function of position
$$[\Phi]_c = -\oint_C \mathbf{E}_s\, ds = 0, \tag{3.12}$$

for an arbitrary contour which may go through the cylinder. In particular,

$$\delta\Phi = \Phi(-\infty, y) - \Phi(\infty, y) = -\lim_{r\to\infty}\int_0^{\pi} rE_\theta\, d\theta = -\lim_{r\to\infty}\int_0^{-\pi} rE_\theta\, d\theta, \tag{3.13}$$

where E_θ is a tangential component of $\mathbf{E}$ along a large circle $x^2 + y^2 = r^2$ given by
$$E_\theta/(\mu H W) = -w\sin\theta + j_\theta/m = -w\sin\theta - (\partial h/\partial r)/m, \tag{3.14}$$

according to (2.14) and (2.15). Introducing (3.2) and (3.7), we obtain

$$\frac{\delta\Phi}{\mu H W} = \lim_{r\to\infty}\int_0^{\pm\pi} r\phi_{\pm}\, d\theta = \frac{\pi}{k}B_{\pm} \tag{3.15}$$

Since $\delta\Phi$ is single valued,
$$B_+ = B_- = B. \tag{3.16}$$

On the other hand, the drag D per unit length of the cylinder is obtained by integrating the mechanical stress τ_{nz} and the Maxwell stress T_{nz} along an arbitrary contour C around the cylinder, i.e.

$$\begin{aligned}\frac{D}{\rho\nu W} &= -\frac{1}{\rho\nu W}\oint_C (\tau_{nz}+T_{nz})\,ds \\ &= -\frac{1}{\rho\nu W}\oint_C \left[\rho\nu\frac{\partial v_z}{\partial n}+\mu H H_z\cos(n,y)\right]ds \\ &= -\oint_C (\partial w/\partial n)\,ds + m\oint_C h\,dx. \end{aligned} \tag{3.17}$$

Choosing as C the above-mentioned large circle, and making use of (3.2)–(3.7) and (3.15)–(3.16), we get

$$D/(\rho\nu W) = \lim_{r\to\infty} m\int_0^{2\pi} r(\phi_+ + \phi_-)\,d\theta = 4\pi B. \tag{3.18}$$

Comparison of (3.15) and (3.18) yields

$$D/(\rho\nu W) = 2m\delta\Phi/(\mu H W) = 4\pi B, \tag{3.19}$$

or

$$D = 2\sqrt{(\rho\nu\sigma)}\,\delta\Phi\times\operatorname{sgn}H. \tag{3.20}$$

This is the final result, the relationship between drag and electric potential difference.

Before concluding this section, we add some remarks on the case of the insulating cylinder. Here, we can simplify the analysis by defining functions $F_\pm$ by

$$\phi_\pm = \tfrac{1}{2}(1\mp h_i)F_\pm. \tag{3.21}$$

The functions $F_\pm$ are solutions of (3.3) with conditions

$$F_\pm = 1 \quad \text{on } S \quad \text{and} \quad F_\pm = 0 \quad \text{at infinity}, \tag{3.22}$$

and thus satisfy all conditions except (2.32). This remaining condition is easily satisfied by taking

$$h_i = (Q_+ - Q_-)/(Q_+ + Q_-), \tag{3.23}$$

where

$$Q_\pm = -\oint_S (\partial F_\pm/\partial n)\,ds. \tag{3.24}$$

Then the viscous drag per unit length $D_f = D$ (there is no magnetic drag in this case) is given by

$$D/(\rho\nu W) = -\oint_S (\partial w/\partial n)\,ds = 2Q_+Q_-/(Q_+ + Q_-). \tag{3.25}$$

In the case of the symmetric configuration mentioned at the end of § 2, in which S is symmetric with respect to a generator (as in the case of an elliptic cylinder), (3.23) shows that h_i is zero because Q_+ is equal to Q_-. Then (3.25) reduces to

$$D/(\rho\nu W) = Q = Q_+ = Q_-. \tag{3.26}$$

Thus, the problem for an insulator has been reduced to a more familiar boundary-value problem of the type (3.3) and (3.22), (or to (3.27) and (3.28) below), and these solutions are easily transferable to our problem.

For example, we consider the case of the flat plate $|x| < a, y = 0$. Putting $\tilde{\phi}_+ = \frac{1}{2}\phi$ in (3.6) (i.e. $h_i = 0, F_+ = \phi \exp(ky)$ in (3.21)), equation (3.3) yields a Helmholtz equation for ϕ

$$(\nabla^2 - k^2)\phi = 0. \tag{3.27}$$

This leads to the same boundary-value problem as in Rayleigh's problem (Hasimoto 1951) for a non-conducting fluid, since

$$\phi = \exp(-ky) = 1 \quad \text{for} \quad y = 0 \quad \text{and} \quad |x| \leqslant a, \tag{3.28}$$

and

$$\phi = O(e^{-kr}) \quad \text{as} \quad r \to \infty. \tag{3.29}$$

We will study this case and the case of a perfectly conducting plate at some length in the following sections.

4. Flat plate of finite width: $|x| \leqslant a, \quad y = 0$

Introducing ϕ, determined by (3.27)–(3.29), into (3.2) we get

$$w = \phi \cosh ky, \tag{4.1}$$

$$h = -\phi \sinh ky = -w \tanh ky, \tag{4.2}$$

where we have used the symmetry of ϕ with respect to $y = 0$

$$\phi(x, y) = \phi(x, -y), \quad \text{i.e. } \tilde{\phi}_+ = \tilde{\phi}_-. \tag{4.3}$$

In particular, at $y = 0$,

$$w = \phi \quad (= 1 \quad \text{for} \quad |x| < a), \quad h = 0, \tag{4.4}$$

$$\omega = \partial w/\partial y = \partial \phi/\partial y \quad (= 0 \quad \text{for} \quad |x| > a), \tag{4.5}$$

$$j_x = \partial h/\partial y = -k\phi, \quad j_y = -\partial h/\partial x = 0. \tag{4.6}$$

Equations (4.6), (2.14) and (2.15) show that the electric current density and the electric field on both sides of the insulating plate are given by

$$J_x = -\tfrac{1}{2}\sigma\mu H W = -\sigma E_x = \sigma E_x', \quad E_y = E_y' = 0 \tag{4.7}$$

exactly, since $w = \phi = 1$ on the plate. The negative sign of σE_x represents the electromotive action of the plate, and assures the satisfaction of the condition (3.12).

Let us proceed to the case of a perfectly conducting flat plate. We put

$$\phi_\pm = \tfrac{1}{2}(\phi \mp \psi)\exp(\pm ky), \tag{4.8}$$

where

$$(\nabla^2 - k^2)\psi = 0. \tag{4.9}$$

The function ψ is antisymmetric with respect to $y = 0$

$$\psi(x, y) = -\psi(x, -y). \tag{4.10}$$

Then, from (3.2),

$$w = \phi \cosh ky - \psi \sinh ky, \tag{4.11}$$

$$h = -\phi \sinh ky + \psi \cosh ky. \tag{4.12}$$

In particular

$$w(x, 0) = \phi(x, 0), \tag{4.13}$$

$$h(x, 0) = \psi(x, 0) \quad (= 0 \quad \text{for} \quad |x| > a). \tag{4.14}$$

According to (4.13) we may use the same function ϕ as that in the insulating case. Also, on the plane $y = 0$,

$$\omega = \partial w/\partial y = \partial\phi/\partial y - k\psi \quad (= 0 \quad \text{for} \quad |x| > a), \tag{4.15}$$

$$j_x = \partial h/\partial y = -k\phi + \partial\psi/\partial y, \tag{4.16}$$

$$j_y = -\partial h/\partial x = -\partial\psi/\partial x \quad (= 0 \quad \text{for} \quad |x| > a). \tag{4.17}$$

Taking into account (2.16), (2.17), (2.30) and (4.17), we get the boundary conditions for ψ

$$\partial\psi/\partial y = k \quad \text{for} \quad |x| < a, \quad y = 0 \tag{4.18}$$

$$\psi = O(e^{-kr}) \quad \text{as} \quad r \to \infty. \tag{4.19}$$

We have now reduced the two flat-plate problems to two kinds of standard boundary-value problems involving the Helmholtz equation for ϕ and ψ.

For the sake of simplicity, we shall consider two important quantities from the practical point of view, i.e. the skin frictional drag $D_f(x)$ and the magnetic drag $D_m(x)$ at a point of the plate, denoting by suffixes I and C corresponding quantities for the insulating and perfectly conducting cases, respectively. The total drag obtained by integrating these drags is intimately related to the induction potential difference $\delta\Phi$ or wake strength B according to (3.19).

We obtain from (4.5) and (4.4)

$$D_{fI}(x)/(\rho\nu W) = -2\omega(x, +0) = -2(\partial\phi/\partial y)_{y=+0} \tag{4.20}$$

and

$$D_{mI}(x) = 0, \tag{4.21}$$

applying (3.17) on the surface element of the plate at x. In the same manner

$$D_{fC}(x)/(\rho\nu W) = -2(\partial\phi/\partial y)_{y=+0} + m\psi(x, +0) \tag{4.22}$$

and

$$D_{mC}(x)/(\rho\nu W) = -2m\psi(x, +0) \tag{4.23}$$

from (4.15) and (4.14). The drag $D_{mC}(x)$ is simply the force acting on the electric current $h(x, +0) - h(x, -0)$ in the perfectly conducting plate. Equations (4.20)–(4.23) afford an exact relation between the two cases

$$D_{fI}(x) = D_{fC}(x) + \tfrac{1}{2}D_{mC}(x) \quad \text{or} \quad D_I(x) = D_C(x) - \tfrac{1}{2}D_{mC}(x). \tag{4.24}$$

The solutions of our two plate problems have been discussed by many authors in many branches of mathematical physics. The following expansion formulae for small and large values of M are obtained from their work

$$\begin{aligned}-\frac{\partial}{\partial y}\phi\,(a\cos\alpha, +0) = \frac{1}{\sin\alpha}\Bigg[&\frac{D_I}{2\pi\rho\nu W} - \frac{M^2}{16}\left(1 - \frac{1}{2\Omega}\right)\cos 2\alpha - \frac{M^4}{256}\left\{\left(\frac{1}{3} + \frac{1}{2\Omega}\right)\cos 2\alpha\right.\\ &\left. + \left(\frac{1}{24} - \frac{1}{32\Omega}\right)\cos 4\alpha\right\} + \frac{M^6}{4096}\left\{\left(\frac{\Omega}{8} + \frac{13}{64} + \frac{11}{16\Omega} - \frac{1}{16\Omega^2}\right)\cos 2\alpha\right.\\ &\left. - \left(\frac{1}{40} + \frac{1}{32\Omega}\right)\cos 4\alpha - \left(\frac{1}{960} - \frac{1}{1152\Omega}\right)\cos 6\alpha\right\} + O(M^8)\Bigg],\end{aligned} \tag{4.25}$$

$$\frac{D_I}{\rho\nu W} = 2\pi\left[\frac{1}{\Omega}\left(1 - \frac{M^2}{16}\right) + \frac{M^4}{1024}\left(1 + \frac{3}{4\Omega} - \frac{1}{2\Omega^2}\right) + \frac{M^6}{49152}\left(1 + \frac{29}{12\Omega} + \frac{3}{2\Omega^2}\right) + O(M^8)\right] \tag{4.26}$$

$$= 2M + 2 - \frac{4}{\pi}[K_{01}(M) - K_{02}(M)] + O(e^{-2M}), \tag{4.26'}$$

$$-\psi(a\cos\alpha,\,+0) = \frac{M}{4\sin\alpha}\left[\frac{2D_{mC}}{\pi M^2\rho\nu W} - \cos 2\alpha + \frac{M^2}{16}\{(\Omega+\tfrac{5}{6})\cos 2\alpha - \tfrac{1}{12}\cos 4\alpha\}\right.$$
$$\left. - \frac{M^4}{256}\{(\Omega^2+\tfrac{11}{8}\Omega+\tfrac{33}{64})\cos 2\alpha - (\tfrac{1}{8}\Omega+\tfrac{13}{160})\cos 4\alpha + \tfrac{1}{320}\cos 6\alpha\} + O(M^6)\right], \tag{4.27}$$

$$\frac{D_{mC}}{\rho\nu W} = 2\pi\left[\frac{M^2}{4} - \frac{M^4}{64}(\Omega+\tfrac{3}{4}) + \frac{M^6}{1024}(\Omega^2+\tfrac{5}{4}\Omega+\tfrac{7}{16}) + O(M^8)\right]. \tag{4.28}$$

$$= 4M - 4 + \frac{8}{\pi}[K_{01}(M)+K_{02}(M)] + O(e^{-2M}), \tag{4.28'}$$

where
$$M = ma = 2ka = \sqrt{\{\sigma/(\rho\nu)\}}\,\mu\,|H|\,a, \tag{4.29}$$

$$\Omega = -\gamma - \log(M/8), \quad \gamma = 0{\cdot}5772\ldots(\text{Euler's const.}), \tag{4.30}$$

$$K_{01}(M) = \int_M^\infty K_0(x)\,dx \sim \sqrt{\frac{\pi}{2M}}\,e^{-M}\left(1 - \frac{5}{8M} + \frac{129}{128M^2} - \ldots\right), \tag{4.31}$$

$$K_{02}(M) = \int_M^\infty K_{01}(x)\,dx = M[K_1(M) - K_{01}(M)]$$
$$\sim \sqrt{\frac{\pi}{2M}}\,e^{-M}\left(1 - \frac{9}{8M} + \frac{345}{128M^2} - \ldots\right). \tag{4.32}$$

We have used a result by Hasimoto (1951) for (4.25), and transformed Levine's result (1957) for Rayleigh's problem into the convenient form (4.26′), where the first two terms have been obtained by Howarth (1950) and by the author (Hasimoto 1951). Equation (4.27) has been calculated by use of the integro-differential equation

$$\left(\frac{\partial\psi}{\partial y}\right)_{y=0} = \frac{1}{\pi}\left(\frac{d^2}{dx^2} - k^2\right)\int_{-a}^{a} K_0(k\,|x-x_0|)\,\psi(x_0)\,dx_0 = k, \tag{4.33}$$

or an integral equation

$$\int_{-a}^{a} K_0(k\,|x-x_0|)\,\psi(x_0)\,dx_0 = -(\pi/k)(1 - A\cosh kx) \tag{4.34}$$

for $\psi(x,0)$ and an unknown constant A subject to the condition

$$\psi(\pm a, 0) = 0, \tag{4.35}$$

which is found to be essentially the same as that discussed in diffraction theory (Bowkamp 1954). Equation (4.28′) was derived by use of Levine's technique (1957), initially applied to (4.26′), although the first two terms of (4.26′) can be easily determined from the results in the next section, where we also give the form of $(\partial\phi/\partial y)_{y=0}$ and $\psi(x,0)$ for large M. Table 1 and figure 2 give the numerical values of D_f and D_m calculated by these formulae.

We notice the following points.

(1) The matching of the two types of approximate formulae, especially for D_I, is good for intermediate values of M.

(2) $D_{fI} > D_{fC}$, but
$$D_I = D_{fI} < (D_f + D_m)_C = D_C. \tag{4.36}$$

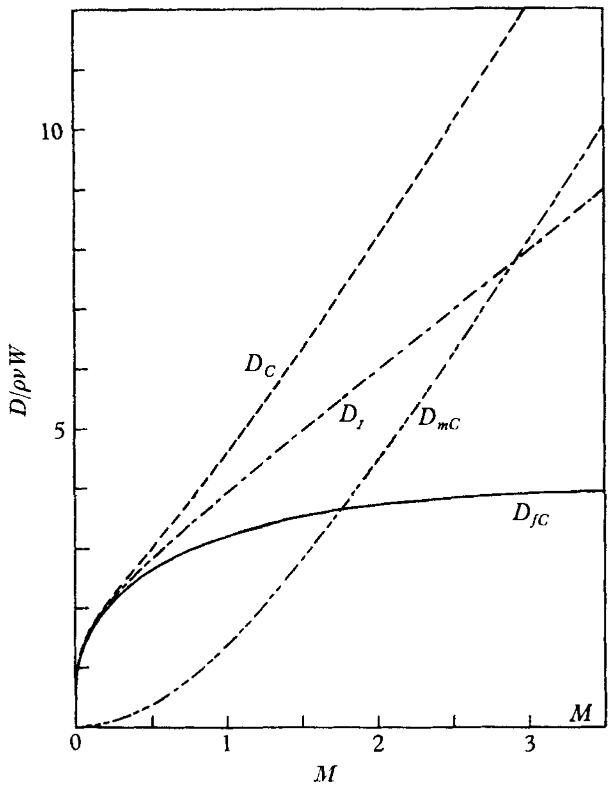

FIGURE 2. Total drag for the finite plate.

M	Perfect conductor $D_f/(\rho\nu W)$		$D_m/(\rho\nu W)$		$D/(\rho\nu W)$		Insulator $D/(\rho\nu W)$	
	Eqs. (4.28), (4.28′)						Eqs. (4.26), (4.26′)	
0·01	0·940	—	0·00016	—	0·940	—	0·940	—
0·05	1·395	—	0·00390	—	1·399	—	1·397	—
0·1	1·64	—	0·0167	—	1·66	—	1·65	—
0·2	1·98	—	0·062	—	2·04	—	2·01	—
0·4	2·45	—	0·24	—	2·69	—	2·57	—
0·6	2·79	—	0·53	—	3·32	—	3·05	—
0·8	3·04	—	0·91	—	3·96	—	3·50	—
1·0	3·24	—	1·38	—	4·62	—	3·93	3·93
1·2	3·39	$3{\cdot}3_5$	$1{\cdot}9_1$	$2{\cdot}0_0$	5·30	$5{\cdot}3_5$	4·35	4·35
1·4	$3{\cdot}5_1$	$3{\cdot}4_9$	$2{\cdot}5_1$	$2{\cdot}5_4$	$6{\cdot}0_2$	$6{\cdot}0_3$	4·76	4·76
1·6	$3{\cdot}5_9$	$3{\cdot}6_0$	$3{\cdot}1_6$	$3{\cdot}1_4$	$6{\cdot}7_6$	$6{\cdot}7_4$	5·17	5·17
1·8	$3{\cdot}6_4$	$3{\cdot}6_8$	$3{\cdot}8_8$	$3{\cdot}7_9$	$7{\cdot}5_2$	$7{\cdot}4_7$	5·58	5·58
2·0	$3{\cdot}6_6$	$3{\cdot}7_5$	—	$4{\cdot}4_7$	—	$8{\cdot}2_2$	5·99	5·99
2·4	—	3·84	—	5·89	—	9·74	—	6·79
2·8	—	3·90	—	7·39	—	11·29	—	7·60
3·0	—	3·92	—	8·15	—	12·07	—	8·00
3·2	—	3·95	—	8·92	—	12·86	—	8·39
3·6	—	3·96	—	10·48	—	14·44	—	9·20
4·0	—	3·97	—	12·05	—	16·03	—	10·00

TABLE 1. The total drag for a finite plate.

(3) For small M, D_{mC} is small since it is $O(M^2)$. In fact

$$D_{mC}/(\rho\nu W) = \tfrac{1}{2}\pi M^2 + O(M^4) \tag{4.37}$$

and, indeed, is so small that D_I and D_C are given by the same formula

$$D_I = D_C = 2\pi/\Omega + O(M^2). \tag{4.38}$$

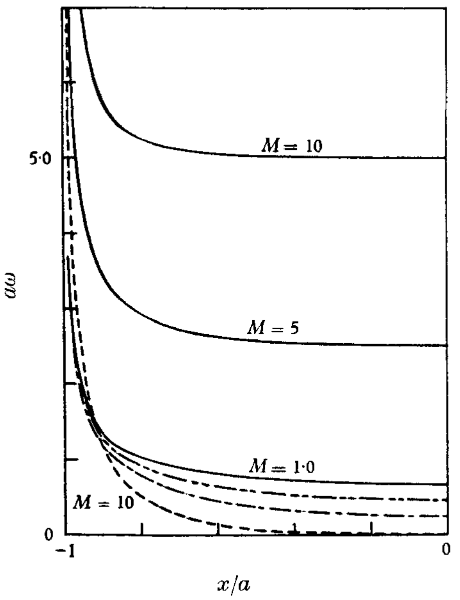

FIGURE 3. Non-dimensional vorticity distribution on the plate. —, Insulator. $a\omega_C$: — - - —, $M = 1$; — - —, $M = 5$; - - - - $M = 10$.

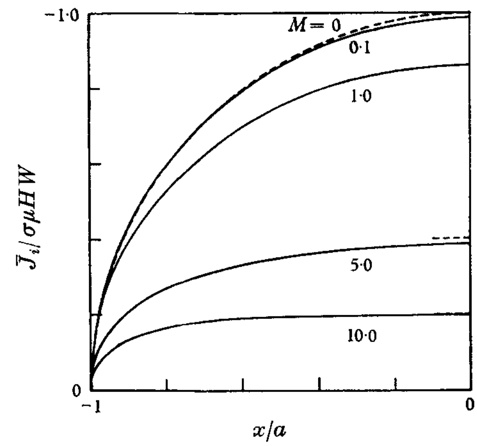

FIGURE 4. Electric current in the perfectly conducting plate.

This is explained by the fact that the current in the plate is so small that its effect on the field in the fluid is negligible.*

(4) For large M (e.g. $M > 3$), the following formulae give good approximations

$$D_I/(\rho\nu W) = 2M + 2, \tag{4.39}$$

$$D_{fC}/(\rho\nu W) = 4, \quad D_{mC}/(\rho\nu W) = 4M - 4. \tag{4.40}$$

Figures 3 and 4 show, respectively, the vorticity ω on the plate and the electric current $\bar{J}_i(x)$ in the perfectly conducting plate.

* We can easily show that (4.38) is valid for an arbitrary shape of cylinder cross-section and arbitrary ratio of σ_i/σ, if we take as $\frac{1}{2}a$ the electrostatic capacity c of this shape. The analogous results have been derived for Rayleigh's problem in non-conducting fluids, by Batchelor (1954) and by the author (1954). We note that ϕ_+ and ϕ_- are given by

$$2\phi_\pm = 1 - \tfrac{1}{2}\log(Z\bar{Z})/[-\gamma - \log(\tfrac{1}{4}mc)] + O(kr),$$

for small values of kr, where the domain outside of the cylinder is conformally mapped onto the region outside the unit circle $Z\bar{Z} = 1$ in the complex Z-plane, by use of the mapping function

$$x + iy = c\left(Z + \sum_{n=1}^{\infty} c_n Z^{-n}\right).$$

Then, (3.2) and (3.17) yield (4.38).

5. Flat plate of semi-infinite width

Let us consider the case of a flat plate of semi-infinite width at greater length, inasmuch as this case has simple exact solutions and affords an approximate, but clear, picture of the field for the finite plate at large M.

For convenience, we introduce the parabolic co-ordinates (ξ, η)

$$kx = \xi^2 - \eta^2, \quad ky = 2\xi\eta, \quad -\infty < \xi < \infty \quad (\eta \geqslant 0), \tag{5.1}$$

so that

$$kr = \xi^2 + \eta^2, \tag{5.2}$$

as suggested by Lamb's study (1932) of the sound diffraction problem. The coordinate η vanishes on the plate $(0 \leqslant x \leqslant \infty,\ y = 0)$ and the coordinate ξ has opposite signs on the two opposite sides of the axis of x, and is zero on the negative x-axis (figure 5).

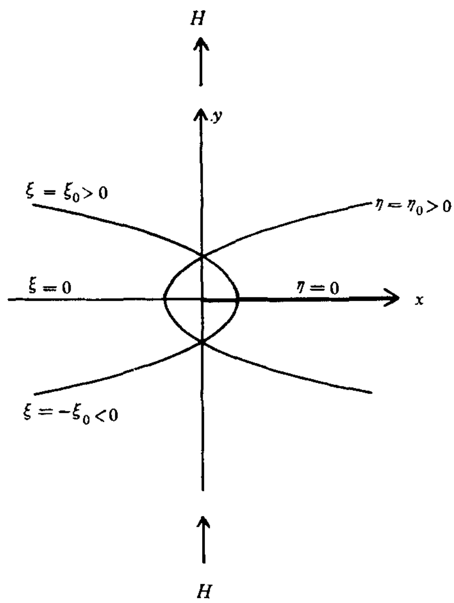

FIGURE 5. Parabolic co-ordinates.

Then (3.3) is transformed to

$$\left(\frac{\partial^2}{\partial\xi^2} + \frac{\partial^2}{\partial\eta^2} \mp 4\eta\frac{\partial}{\partial\xi} \mp 4\xi\frac{\partial}{\partial\eta}\right)\phi_\pm = 0 \tag{5.3}$$

which is satisfied by

$$\phi_\pm = E_0(\eta \mp \xi), \tag{5.4}$$

where E_0 is the complementary error function

$$E_0(\zeta) = \operatorname{erfc}\zeta = 1 - \operatorname{erf}\zeta = \frac{2}{\sqrt{\pi}}\int_\zeta^\infty e^{-\zeta^2}\,d\zeta. \tag{5.5}$$

We can construct from (5.4) two solutions of the Helmholtz equations which are symmetric and antisymmetric with respect to $y = 0$, taking into account (3.4), (3.6) and (5.1):

$$\left.\begin{matrix}\phi\\ \psi\end{matrix}\right\} = \tfrac{1}{2}[e^{ky}E_0(\eta + \xi) \pm e^{-ky}E_0(\eta - \xi)]. \tag{5.6}$$

Fortunately, these satisfy all the conditions required for ϕ and ψ in the previous section, if, by considering the infinite extent of the plate, we replace $|x| \leqslant a$ by $0 \leqslant x \leqslant \infty$ and $r \to \infty$ by $\eta \to \infty$ in (3.29) or (4.19). We can easily establish this solution by taking into account the symmetry of $E_0(\eta-\xi)$ and $E_0(\eta+\xi)$, and the results

$$E_0(-\xi)+E_0(\xi) = 2, \tag{5.7}$$

$$E_0(\zeta) \sim e^{-\zeta^2}/(\sqrt{(\pi)}\,\zeta) \quad \text{or} \quad 2, \quad \text{as} \quad \zeta \to +\infty \quad \text{or} \quad -\infty, \tag{5.8}$$

$$\frac{\partial}{\partial y}E_0(\eta \pm \xi) = \frac{1}{2r}\left(\eta\frac{\partial}{\partial \xi}+\xi\frac{\partial}{\partial \eta}\right)E_0 \to -\sqrt{\frac{k}{\pi x}}\,e^{-\xi^2} \quad \text{as} \quad \eta \to 0. \tag{5.9}$$

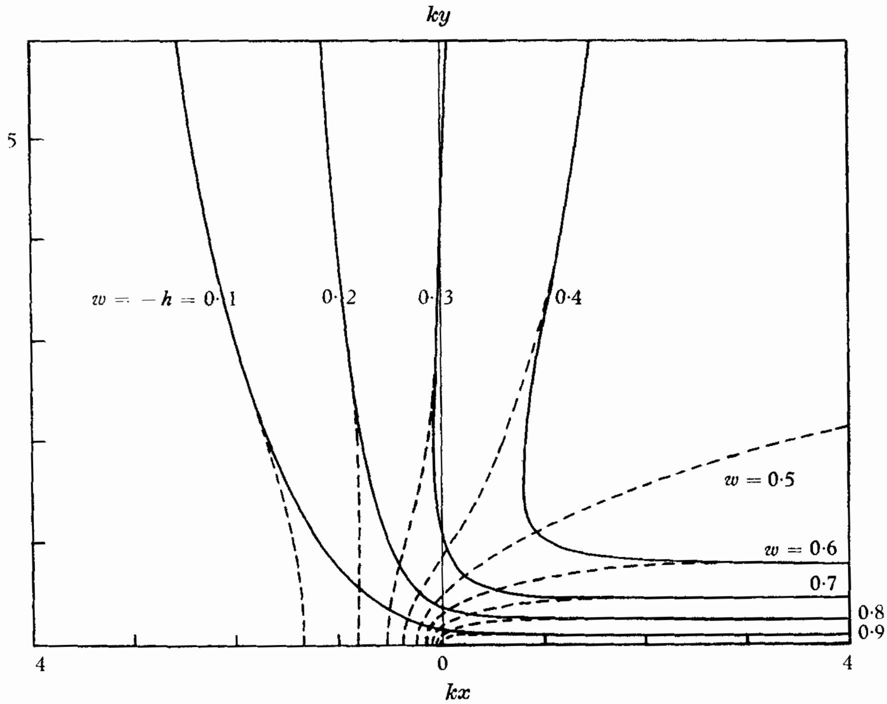

FIGURE 6. Field for the insulating semi-infinite plate. - - - -, $w =$ const.; —, $h =$ const.

Let us proceed to the discussion of the exact solutions constructed in this way for the two extreme cases.

5.1. *The insulating plate*

From (4.1), (4.2) and (5.6) we get

$$\left.\begin{matrix} w \\ -h \end{matrix}\right\} = \frac{1}{2}\left\{\begin{matrix}\cosh ky \\ \sinh ky\end{matrix}\right\}[e^{ky}E_0(\eta+\xi)+e^{-ky}E_0(\eta-\xi)]. \tag{5.10}$$

Figure 6 shows the distribution of the isovels ($w =$ const.) and electric current lines $h =$ const. We have only to consider the positive y-plane since w is symmetric and h is antisymmetric with respect to $y = 0$.

From this analysis, the interesting points are as follows.

(1) There is a boundary layer on the plate, as shown by

$$\lim_{\xi\to\infty}\frac{w}{h} = \tfrac{1}{2}(e^{-my}\pm 1) \tag{5.11}$$

for fixed positive values of η. It is interesting that the values of w and $-h$ tend to $\frac{1}{2}$ in a wide region outside this boundary layer.

(2) There is a transition region of vague parabolic shape for large ky between the above-mentioned region (core) and the undisturbed region represented by $\eta\to\infty$. This also is shown by (5.8) and

$$w = -h \to \phi_+ = \tfrac{1}{4}E_0(\zeta)+O(1/\sqrt{(kr)}) \quad \text{as} \quad \xi,\eta\to\infty, \tag{5.12}$$

where

$$\zeta = \eta-\xi, \quad y = \tfrac{1}{2}k[(x/\zeta)^2-(\zeta/k)^2]. \tag{5.13}$$

We note that the current lines coincide with isovels for large ky, where (3.10) is valid. On the line $x = 0$ ($\xi = \eta$), we get

$$\left.\begin{matrix} w \\ -h \end{matrix}\right\} = \tfrac{1}{4}(1\pm e^{-my})\,[1+e^{my}E_0(2\sqrt{(ky)})] \sim \tfrac{1}{4}+O\left(\frac{1}{\sqrt{(ky)}}\right). \tag{5.14}$$

The value $\frac{1}{4}$ is the mean of their values; $\frac{1}{2}$ in the core, and zero in the undisturbed region. This region is rather narrow compared with the width of our plate and is shifted outward to the undisturbed region for moderate values of ky. We might call this region a shear layer.

(3) For $HW < 0$, the main part of the electric current comes from $ky = \infty$, along isovels in the shear layer, and go into the other isovels in the plate boundary layer parallel to the plate for large kx. For $HW > 0$, this direction is reversed.

(4) In the vicinity of the edge, isovels take parabolic shapes given by

$$1-w \sim 2\eta/\sqrt{\pi}. \tag{5.15}$$

Here, the electric current lines are almost parallel to the plate

$$h \sim -ky, \tag{5.16}$$

corresponding to (4.6), (4.7) and (5.11).

5.2. *The perfectly conducting plate*

Introducing (5.6) into (4.11) and (4.12) we get simple expressions

$$\left.\begin{matrix} w \\ -h \end{matrix}\right\} = \tfrac{1}{2}\,[E_0(\eta-\xi)\pm E_0(\eta+\xi)]. \tag{5.17}$$

This equation could have been constructed from (5.4) directly. Figure 7 shows the field in this case. We can notice the symmetry between w and $1-|h|$ with respect to the y-axis

$$w(x,y)+|h(-x,y)| = 1, \tag{5.18}$$

derived from (5.17), (5.7) and (5.1).

We may remark that:

(1) There is no boundary layer on the plate except near the edge $kx \ll 1$, and the fluid is moving with almost the same speed as the plate for a wide core region, as shown by

$$\lim_{\xi\to\infty} w \sim -\lim_{\xi\to\infty} h = 1 \quad \text{for fixed } \eta. \tag{5.19}$$

(2) The strengths of the vorticity and the current in the shear layer have values twice those of the insulating case, and the shear layer is more distinct than that case. This is shown by (5·8) and

$$w \sim -h \sim \tfrac{1}{2}E_0(\zeta) \quad \text{for} \quad \xi, \eta \gg 1. \tag{5.20}$$

In the distinct centre of this layer ($x = 0$) w and $-h$ have values which are the mean of their values in the core and their values in the undisturbed region, i.e. $\frac{1}{2}$.

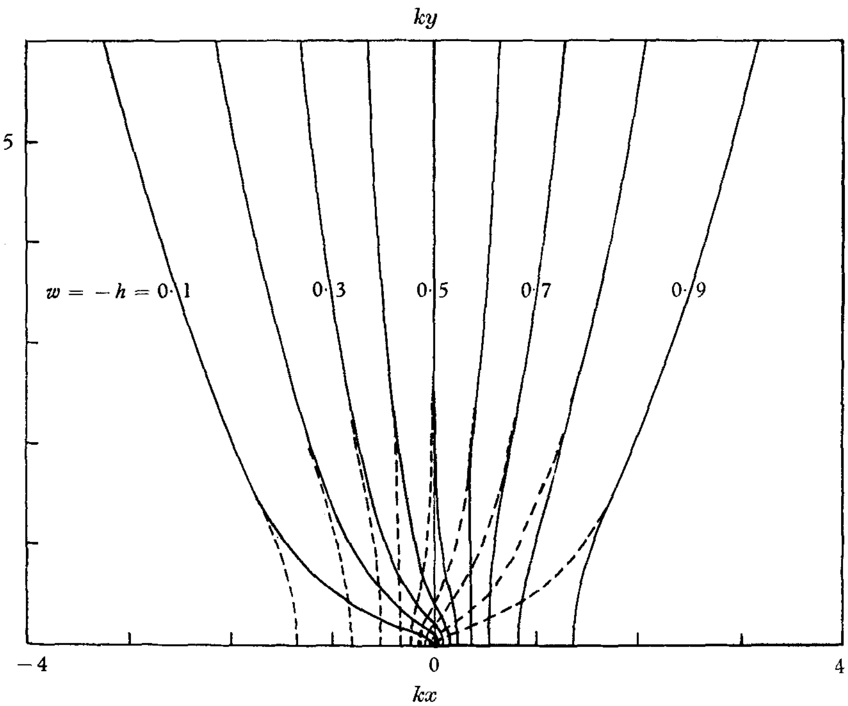

FIGURE 7. Field for the perfectly conducting semi-infinite plate.
- - - -, w = const.; —, h = const.

(3) The electric current from the shear layer enters the plate perpendicularly, almost at the edge of the plate, and flows in the plate to $kx = +\infty$, if HW is negative. This electric current and the induced magnetic field on the plate are given by

$$\left.\begin{aligned} j_y &= -\omega = \sqrt{\{k/(\pi x)\}}\exp(-kx), \quad &(5.21)\\ -h &= 1 - E_0(\xi) = \operatorname{erf}(\sqrt{(kx)}). \quad &(5.22)\end{aligned}\right\} \text{ for } \quad y = +0.$$

Equations (2.13), (2.15) and (5.22) show that the total electric current $\bar{J}_i$ in the plate is given by

$$\bar{J}_i/(\sigma\mu HW) = m^{-1}[h(x, +0) - h(x, -0)] = -(2/m)\operatorname{erf}\sqrt{kx} \tag{5.23}$$

which grows from zero at $x = 0$ to $2\sqrt{(\rho\nu\sigma)}\,W$ at $kx = \infty$ gathering all the electric currents from the fluid (for $HW < 0$) (figure 4). $\sqrt{(\rho\nu\sigma)}\,W$ is equal to the total current in the upper shear layer $m^{-1}\sigma\mu HW[h_{(x=-\infty)} - h_{(x=+\infty)}]$.

(4) In the vicinity of the edge, isovels and current lines form orthogonal parabolic nets

$$1-w \sim 2\eta/\surd\pi, \quad h \sim -2\xi/\surd\pi, \tag{5.24}$$

which should be compared with (5.15) and (5.16).

6. Discussion for the cylinder of finite width at large Hartmann number

The quantities on the plate $y = 0$ derived from the previous section are simple expressions and are useful in the rest of the paper. They are given in table 2, wherein the lower sign of $\mp$ denotes the value for $y = -0$ (the under side of the plate). The following notation is also used in Table 2.

$$\left.\begin{aligned} E_n &= \int_\xi^\infty E_{n-1}(\xi)\,d\xi, \quad \xi = \surd(k|x|),\\ E_1 &= \frac{1}{\surd\pi}e^{-\xi^2} - \xi E_0 \sim \begin{cases} 1/\surd\pi & \text{for} \quad \xi = 0,\\ \tfrac{1}{2}e^{-\xi^2}/(\surd(\pi)\,\xi^2) & \text{for} \quad \xi \gg 1,\end{cases}\\ E_2 &= \tfrac{1}{4}E_0 - \tfrac{1}{2}\xi E_1 \sim \begin{cases} \tfrac{1}{4} & \text{for} \quad \xi = 0,\\ \tfrac{1}{4}e^{-\xi^2}/(\surd(\pi)\,\xi^3). \end{cases}\end{aligned}\right\} \tag{6.1}$$

	(I) Insulator		(II) Perfect conductor	
	$x<0$	$x>0$	$x<0$	$x>0$
w	E_0	1	E_0	1
h	0	0	0	$\mp(1-E_0)$
ω	0	$\mp(k+\surd(k/x)E_1)$	0	$\mp\surd\{k/(\pi x)\}\,e^{-kx}$
j_x	$-kE_0$	$-k$	$-\surd(k/\lvert\pi x\rvert)\,e^{-k\lvert x\rvert}$	0
j_y	0	0	0	$-\omega$
$E_x/(\mu HW)$	$\frac{1}{2}E_0$	$\frac{1}{2}$	E_0+j_x/m	1
$E_y/(\mu HW)$	0	0	0	$-\omega/m$
$\dfrac{\Phi-\Phi(-\infty,0)}{\mu HW}$	$\dfrac{1}{m}(2E_2-E_0)\leqslant 0$	$-\dfrac{1}{2m}(1+mx)$	$\dfrac{1}{m}(4E_2-E_0)\leqslant 0$	$-x$
$D_{fx}/(\rho\nu W)$	0	$1+mx-4E_2$	0	$2-2E_0$
$D_{mx}/(\rho\nu W)$	0	0	0	$2mx-2-(8E_2-4E_0)$

TABLE 2. Quantities on the semi-infinite plate.

Equations (6.1)–(6.3) are tabulated in the book of Carslaw & Jaeger (1947). D_{fx} is the total frictional drag on the plate between o and x, and D_{mx} is the corresponding magnetic drag

$$D_{fx} = -2\rho\nu W\int_0^x \omega\,dx, \tag{6.2}$$

$$D_{mx} = -2m\rho\nu W\int_0^x h\,dx. \tag{6.3}$$

Except for Φ and D we can separate the quantities on the plate into two terms: one which is constant everywhere (e.g. k in the ω term) and the other which is significant only at the edge and tends to zero rapidly as $kx \to \infty$ (e.g. $\surd(k/x)\,E_1$, in the ω term). If we limit our plate by another edge at $x = 2a$, and superpose the contribution due to this edge, we may obtain a picture of the field near the plate of finite width $2a$ at large Hartmann number $M = ma$. In the quantities D and Φ, the integrals of ω, h and E_x, the contributions due to an edge appear as constants. For example, the total frictional drag and the total magnetic drag for the finite plate are

$$D_{fI}/(\rho\nu W) \sim 2M+1+1 = 2M+2, \quad D_{mI} = 0 \tag{6.4}$$

in the case of an insulator, and

$$D_{fC}/(\rho\nu W) \sim 2+2 = 4, \quad D_{mC}/(\rho\nu W) = 4M-2-2 = 4M-4 \tag{6.5}$$

for a perfect conductor, where we have added to $D_{f,2a}$ etc., as they appear in the table, the contributions due to the presence of another edge. We have neglected also small terms like E_n. Equations (6.4) and (6.5) are identical with (4.39) and (4.40). We can also show the validity of (3.20), (4.7), (4.24), etc., by the general theory, using Table 2 and the above argument for the edge correction. For example

$$\delta\Phi_I/(\mu HW) = a+1/m = D_I/(2m\rho\nu W), \tag{6.6}$$

$$\delta\Phi_C/(\mu HW) = 2a = D_C/(2m\rho\nu W) \tag{6.6'}$$

(compare this with (3.20)).

From these results and the results of the previous sections we may easily build up a picture of the field at large but finite M. In the following, we proceed to show that our picture is applicable generally to the field around a cylinder ($|x| \leqslant a, f_-(x) < y < f_+(x) f_\pm(x) = O(a)$) at extremely large $M = ma$, if we are not concerned with the fine structure of the field (e.g. at an edge $x = a$ on S). We may suppose, according to (2.11) that the fluid has low viscosity and high conductivity and that the applied field is strong. We also assume HW to be negative for convenience.

6.1. *Perfectly conducting cylinder*

In this case the cylinder carries magnetic lines of force frozen in it corresponding to the induction current in the x-direction accompanying its motion. This movement of magnetic lines will drag the fluid in the region $|x| < a, y < \infty$, (i.e. the core) with the same velocity as the cylinder, since the fluid is highly conducting. Then, putting $m = \infty$ in (2.14), we find that the electric field in this region is $E_x = \mu HW$, $E_y = 0$. Taking into account (3.13) and the fact that $E = 0$ in the undisturbed region $|x| > a$, we find that (6.6′) is valid in our general case. The viscous drag is also negligible.

We may note that this picture is perfectly consistent with the fundamental equations and boundary conditions (2.8), (2.9) and (2.30) in the limit of $m \to \infty$, except for the conditions at $y = \infty$ and $|x| = a$. By adding to this picture wakes ((3.7′), (3.15) and (3.16)) for $y \to \infty$, and shear layers of thickness $O(\surd(ky)/k) = O(\surd(y/m))$ (see (5.20)) due to the presence of the viscosity and the finite conductivity, we can satisfy all the conditions required. Taking into account (3.2), (3.10) and $w = 1$, valid in the core, we find that $h = 1$ in the upper core. According to this result, the electric current in the core is negligibly small compared with the current in the cylinder starting from an edge at $x = -a$ and goes into the other edge at $x = a$, owing to the assumption $\sigma_i/\sigma = \infty$. We find that this current forms a closed circuit around the core. This circuit consists of the cylinder (playing the role of a motor with terminals at $x = \pm a$), shear layers (across which h jumps from 0 to ∓ 1) and wakes at infinity (where current lines coincide with isovels elongated in the direction of the applied field).

6.2. *Insulating cylinder*

In this case there is no induction current in the cylinder itself. However, the electric current is induced in the fluid dragged by the cylinder through viscosity and confined in $|x| < a$ due to the strong magnetic field. This current will form surface currents of thickness $O(1/[m \cos(n, y)])$ (Shercliff 1953) from $x = -a$ to $x = a$ (figure 8). This surface current will retard the velocity of the fluid and will yield a boundary layer in which the velocity changes from the speed of the cylinder to a core speed which is a definite fraction of the cylinder speed. The field near the edge $|x| < a$ will be complicated in general, on account of the interaction of the boundary layer and shear layer, and will be inflated a little outwards. The general features of the field will be the same as those in the case of a perfect conductor (or the case of a plate in §§ 5 and 6), if we consider the boundary-current layer to be included in the cylinder.

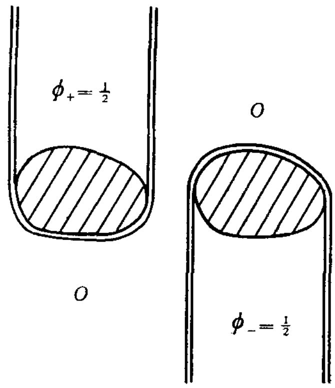

FIGURE 8. Field near the insulating cylinder for extremely large M.

We may show that these features are consistent with the fundamental equations as $m \to \infty$, if we take as the quantities in the core

$$w = \tfrac{1}{2}, \quad h = \mp \tfrac{1}{2}, \tag{6.7}$$

which yield also (6.6), if we neglect small terms $o(ma)$ and take into account (2.14) and (3.13). It is convenient to start from (3.3) and (3.22). Letting $m \to \infty$, we get

$$\phi_+ = \tfrac{1}{2}(1 - h_i) \quad \text{for} \quad \infty > y \geqslant f_-(x) \quad \text{and} \quad |x| < a, \tag{6.8}$$

$$= 0 \quad \text{for} \quad y = \infty, \quad \text{or} \quad |x| > a \cdot \quad \text{or} \quad y < f_-(x) \tag{6.8$'$}$$

(approximation of geometrical optics). The field given by (6.7) (the field in the upper core region and on the cylinder) is connected with the outside undisturbed region given by (6.7) through the wake, the shear layers, and a boundary layer $\phi_+ = \frac{1}{2}(1 - h_i) \exp[-mn\,|\cos(n, y)|]$ on the lower surface of the cylinder (figure 8). A similar solution is obtained for ϕ_- and yields, with ϕ_+, (6.7). By taking a rectangular circuit around the cylinder in equation (3.12), we find that h_i is $o(ma)$.

6.3. *A plate of small thickness $2b$ ($kb \ll 1$) and finite conductivity*

The fields in the core obtained so far seem to be independent of the finite width of the cylinder. The dependency on the finite conductivity is also not clear. As an illustration, we consider the region of the plate far from the edge, where every quantity will be independent of x. In this case $N(P_0; P)$ of (2.26) is given approximately by

$$N(P_0; P) \sim -\tfrac{1}{2}\delta(x_P - x_0)\,|\,y_P - y_0\,|. \tag{6.9}$$

Then

$$h(P_0) = \pm(\sigma_1 b/\sigma)(\partial h/\partial y)_{P_0}, \tag{6.10}$$

approximately, where the first integrals in (2.28) and (2.29) vanish by symmetry. Equation (6.10) can also be obtained from (2.18) and (2.20) by assuming a uniform current, i.e. constant $\partial h_i/\partial y$, in the plate and putting $h_i(P_0)$ equal to $b(\partial h_i/\partial y)$. We find that (4.11)–(4.17) and (4.24) are also valid in this case.

According to table 2, (6.10) is satisfied for large kx by taking a weighted mean of I and II (*c*)

$$(1+\beta)\,h = h_I+\beta h_{II}, \quad (1+\beta)\,w = w_I+\beta w_{II}, \tag{6.11}$$

where

$$\beta = \sigma_i kb/\sigma, \tag{6.12}$$

if we put the x-axis on the upper surface of the plate. Then,

$$\left.\begin{matrix} w \\ -h \end{matrix}\right\} = \frac{1}{2(1+\beta)}[1+2\beta \pm e^{-my}] \quad (mx\to\infty,\ y>0). \tag{6.13}$$

which gives for the fields in the core

$$w_{\text{core}} = -h_{\text{core}} = \tfrac{1}{2}(1+2\beta)/(1+\beta). \tag{6.14}$$

Our perfectly conducting infinitely thin plate is the limiting case in which b is very small but σ_i/σ is extremely large (figure 9).

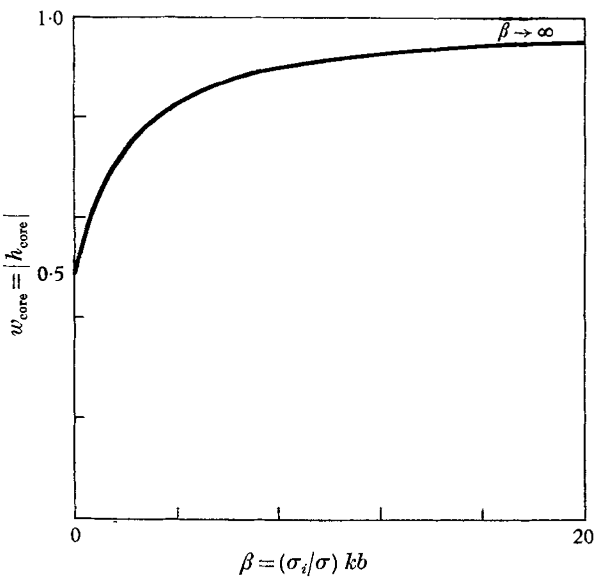

FIGURE 9. Core velocity w_{core} *vs* $(\sigma_i/\sigma)\,kb$.

Let us compare these solutions with the corresponding final stationary solutions in Rayleigh's problem for an infinite flat plate

$$Gw = 1+2\beta+\surd(\kappa/\nu)\,e^{-my}, \quad -G\surd(\nu/\kappa)\,h = 1+2\beta-e^{-my} \tag{6.15}$$

where

$$G = 1+\surd(\kappa/\nu)+2\beta, \quad (y>0). \tag{6.16}$$

We find that:

(1) In general, the two results do not coincide with each other, although they do not contain the width of the plate explicitly. This discrepancy should be reduced to the existence of shear layers in our problem. These layers originate at the edges of the plate and yield finite jumps of field quantities. In the case of

Rayleigh's problem we have no such edges in space, although the time $t = 0$ might play the same role.

(2) It is a remarkable fact that these two results coincide, if the magnetic Prandtl number is 1, i.e. if $\nu = \kappa$. This is the case in which equipartition of the induced magnetic energy and the kinetic energy of the fluid is attained far from the plate (see (3.11)). This is the same feature as that of the wave of finite amplitude in the non-viscous and perfectly conducting fluid (Walén 1942).

In conclusion the author expresses his cordial thanks to Prof. F. H. Clauser and Prof. L. S. G. Kovasznay for their useful suggestions and encouragement, and also to Prof. R. R. Long for his kind help in the revision of the manuscript. The author has been supported by the International Cooperation Administration under the visiting research programme administered by the National Academy of Sciences of U.S.A.

REFERENCES

Batchelor, G. K. 1954 *Quart. J. Mech. Appl. Math.* **7**, 179.

Bleviss, Z. O. 1958 *J. Aero. Sci.* **25**, 601.

Bowkamp, C. J. 1954 *Rep. Prog. Phys.* **17**, 35.

Carslaw & Jaeger 1947 *Conduction of Heat in Solids.* Oxford University Press.

Chang, C. C. & Yen, J. T. 1959 *J. Phys. Fluid*, **2**, 393.

Hartmann, J. 1937 *Math.-Fys. Medd.* **15**, no. 6.

Hasimoto, H. 1951 *Proc. 1st Japan. Nat. Congress Appl. Mech.* (1951) p. 447.

Hasimoto, H. 1954 *J. Phys. Soc. Japan*, **9**, 611.

Howarth, L. 1950 *Proc. Camb. Phil. Soc.* **46**, 127.

Kakutani, T. 1958 *J. Phys. Soc. Japan*, **13**, 1504.

Lamb, H. 1932 *Hydrodynamics*, 6th ed. Cambridge University Press.

Levine, H. 1957 *J. Fluid Mech.* **2**, 145.

Resler, E. L. Jr. & Sears, W. R. 1958 *J. Aero. Sci.* **25**, 235.

Rossow, V. J. 1957 NACA, TN, 3971.

Shercliff, J. A. 1953 *Proc. Camb. Phil. Soc.* **49**, 136.

Shercliff, J. A. 1956 *J. Fluid Mech.* **1**, 644.

Walén, C. 1944 *Ark. Mat. Astr. Fys.* **30**A, 15.